J Mater Sci: Mater Electron (2017) 28:17908–17916
DOI 10.1007/s10854-017-7732-6

Layered PPy/Cr_2O_3 as a supercapacitor electrode with improved electrochemical performance

P. M. Kharade[1] · J. V. Thombare[2] · S. L. Kadam[3] · S. B. Kulkarni[3] · D. J. Salunkhe[1]

Received: 10 April 2017 / Accepted: 16 August 2017 / Published online: 21 August 2017

Abstract In the present work, we have synthesised polypyrrole (PPy), Cr_2O_3 and layered PPy/Cr_2O_3 thin films on stainless steel (SS) substrates for electrochemical supercapacitor applications. The PPy and Cr_2O_3 thin films were deposited by galvanostatic electrodeposition on stainless steel substrate separately. Layered PPy/Cr_2O_3 thin films are prepared via electrochemical polymerization of PPy on which Cr_2O_3 layer was deposited by electrodeposition technique. The structural and surface morphological studies of these thin films were carried out with the help of X-ray diffraction (XRD) technique and scanning electron microscopy (SEM) images. XRD study remarks that formation of crystalline Cr_2O_3 and amorphous PPy while in the layered PPy/Cr_2O_3 structure showed no additional peaks. The formation of polypyrrole in layered PPy/Cr_2O_3 was confirmed by Fourier transform infrared (FTIR) spectroscopy. The SEM images showed favourable morphology for supercapacitive study. Furthermore, the electrochemical supercapacitive properties were studied by cyclic voltammetry (CV), galvanostatic charging–discharging and electrochemical impedance spectroscopy (EIS) techniques. The layered PPy/Cr_2O_3 thin film showed higher coulombic efficiency of 97% and specific power 49.75 kW kg^{-1} at current density of 0.5 mA cm^{-2}. In addition to this, the layered PPy/Cr_2O_3 thin film showed higher cycling stability than that of pure PPy and Cr_2O_3 thin film electrodes. This may be due to outstanding electrochemical properties that are mainly attributed to the synergistic effect between PPy and Cr_2O_3 and its novel architecture.

✉ D. J. Salunkhe
salunkhedj@rediffmail.com

[1] Nano-Composite Research Laboratory, K.B.P.Mahavidyalaya, Pandharpur, MH 413304, India

[2] Department of Physics, Vidnyan Mahavidyalaya, Sangola, MH 413307, India

[3] Department of Physics, Institute of Science, Mumbai, MH 400032, India

1 Introduction

Supercapacitors or ultracapacitors are the electrochemical energy storage device. On the contrary, they store superior energy density than conventional capacitors and better power density than batteries [1]. Along with they have long cycle life, better cycling ability, high efficiency, reversibility and lightweight which make them supercapacitor as a promising energy storage device. They can be used in variety of potential applications such as hybrid electric vehicle [2], uninterruptible power supplies [3], memory back up devices, digital communication [4], etc. Electrochemical capacitors can be classified into two ways based on the charge storage mechanism such as electrical double layer capacitor and pseudocapacitor. The former is named as electrochemical double layer capacitor in which non faradaic reaction happens. The electrode materials used in electrochemical double layer capacitors are carbon. The later is called pseudocapacitors, in which charge storage is done with the help of faradaic reaction [5]. Transition metal oxides and conducting polymers based electrodes are used in pseudocapacitors.

Conducting polymer is a class of smart materials whose conductivity lies between the ranges of metals. The polymers such as polythiophene, polypyrrole and polyaniline are most studied conducting polymers. Among these conducting polymers, polypyrrole is one of the best conducting polymers thanks to availability of monomer, low cost, toxicity, environmental stability, high voltage window, high porosity, high conductivity in doped states and easy synthesis [6–8].

However, they suffer from swelling and shrinking during the intercalation and de-intercalation process. They lead to mechanical degradation of the electrode during the cycling process. Hence they have low cycling stability.

Several transition metal oxides such as RuO_2, MnO_2, Co_3O_4, NiO, Cr_2O_3 etc have been studied for supercapacitor applications [9–13]. The ruthenium oxide (RuO_2) is mostly studied for supercapacitor application which shows maximum specific capacitance of 1500 F g^{-1} [9]. However, high cost and toxic nature of the ruthenium oxide electrode limits its further commercial application. Hence alternative low cost materials such as MnO_x, Co_3O_4, NiOx, and Cr_2O_3 have been studied for supercapacitor with good capacitive performance. Among these metal oxides, Cr_2O_3 is low cost and widely used in many applications such as; catalysts [14–17], magnetic applications [18] and gas sensors [19], pigment [20] wear resistance [21, 22], advanced colorant [23], and solar energy collector [24]. However, Cr_2O_3 electrode has disadvantage of low specific capacitance and conductivity.

Taken consideration to these drawbacks of polypyrrole and Cr_2O_3 in the present view we have decided to make composite of PPy/Cr_2O_3 layered thin film. It is expected that the combination of PPy and chromium oxide will produce synergetic effect. Earlier literature such as MnO_2/PPy [25], Co_3O_4@PPy [26], ZnO–PPy [27], PPy/TiO_2 [28] etc; have been reported and well explained the synergetic effect which is useful for supercapacitor application. As per authors literature survey there is only few availability of report on the synthesis and characterization of layered PPy/Cr_2O_3 composites for supercapacitor application which appears to be promising work.

In the present work, efforts have been taken to synthesize PPy–Cr_2O_3 layered structure using galvanostatic electrodeposition method; so as we can improve electrochemical performance of single material (PPy–Cr_2O_3) from PPy and Cr_2O_3. Such properties will be useful for supercapacitor application like enhancement in coulombic efficiency, specific capacitance, specific energy and specific power than parent electrodes.

2 Experimental

2.1 Synthesis of PPy

The PPy thin films were synthesized following procedure reported earlier by reference [29]. Here, aqueous 0.1 M pyrrole was mixed with aqueous 0.1 M H_2SO_4 and PPy thin films were deposited on stainless steel (SS) substrates via galvanostatic electrodeposition method at constant current density of 5 mA cm^{-2} for 600 s. Prior to deposition, the SS substrates were pre-treated with dilute HCl and rinsed thoroughly with distilled water and acetone. The films grown exhibit black colour indicating formation of PPy.

2.2 Synthesis of Cr_2O_3

The Cr_2O_3 thin films were synthesized using an aqueous bath of 0.5 M $CrCl_3$*$6H_2O$ via cathodic electrodeposition technique. The chromium was deposited on the SS substrates galvanostatically with deposition at constant current density of 10 mA cm^{-2} for 1800 s and then annealed at 450 °C for 1 h in air atmosphere.

2.3 Synthesis of PPy/Cr_2O_3

The layered PPy/Cr_2O_3 thin film were synthesized as follows, the polypyrrole thin film deposited on SS substrate by using above mentioned process was used to form layered PPy/Cr_2O_3 thin film. The chromium was deposited cathodically on polypyrrole thin film at constant current density of 10 mA cm^{-2} for 1800 s. In the present case the formation of Cr layer on polypyrrole thin film was anodically oxidized in 0.5 M KOH bath. Then the deposited PPy, Cr_2O_3 and PPy/Cr_2O_3 thin films were used for various characterization techniques.

2.4 Characterization techniques

The deposited films in the form of layered structure, were characterized by XRD technique for crystallographic study using Bruker axis D8 Advance Model with copper radiation (Kα of λ = 1.54 Å) in the 2θ range from 20° to 80°. The Fourier transform infrared (FTIR) spectrum of the deposited samples were compiled using a 'Perkin Elmer, FTIR Spectrum one' unit. The surface morphology was studied using SEM, JEOL JSM 6390. The cyclic voltammetry, electrochemical stability and galvanostatic charging–discharging studies were carried out using electrochemical workstation (CHI 660C). The EIS study was evaluated using the electrochemical workstation (CHI 660C). An electrochemical cell was constituted using three electrode systems, deposited film as a working electrode, graphite as a counter electrode and saturated calomel electrode (SCE) as a reference electrode. The aqueous 0.5 M Na_2SO_4 was used as an electrolyte for electrochemical supercapacitor cell.

3 Results and discussions

3.1 XRD studies

For the structural detection of the PPy, Cr_2O_3 and layered PPy/Cr_2O_3 thin films, XRD was carried out in the 2θ range between 20° and 80°. Figure 1a–c show the XRD patterns

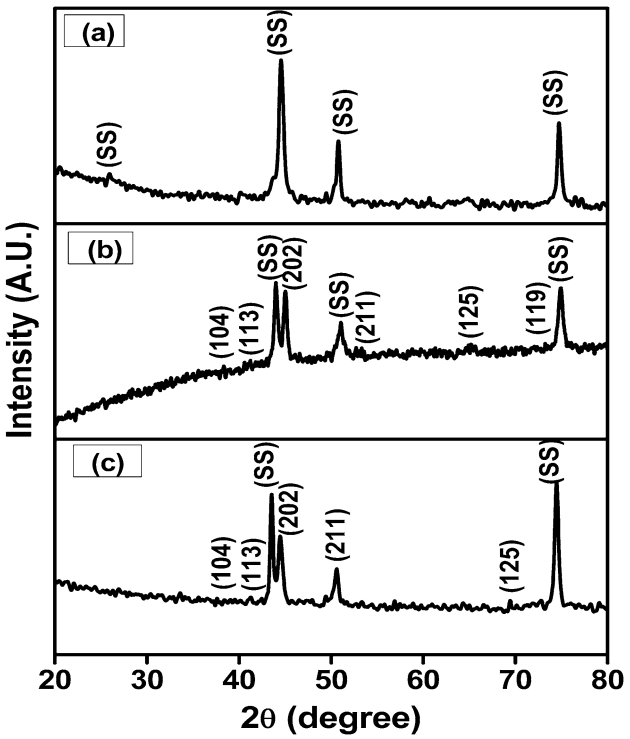

Fig. 1 X-ray Diffraction pattern of **a** PPy thin film, **b** Cr_2O_3 thin film and **c** PPy/Cr_2O_3 thin film

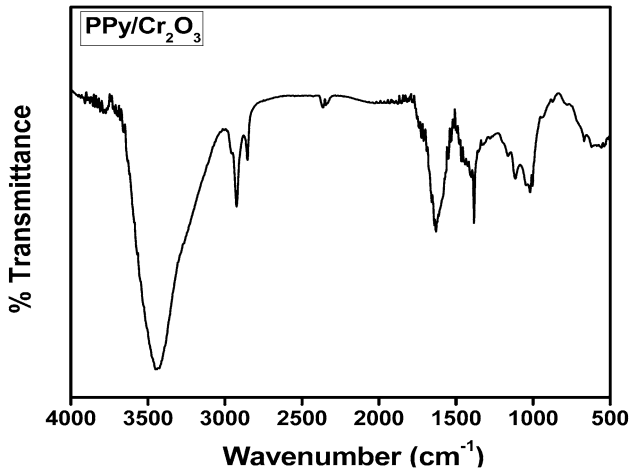

Fig. 2 Fourier transform infrared (FTIR) spectroscopy of layered PPy/Cr_2O_3 thin film

of PPy, Cr_2O_3, and PPy/Cr_2O_3 thin films deposited on SS substrates. Figure 1a shows the XRD spectra of polypyrrole thin films which do not show any characteristic broad peak. Observed peaks are due to SS substrate only. The XRD pattern confirms that the amorphous nature of polypyrrole thin film which is consistent with XRD pattern of PPy observed by other group [30, 31]. Furthermore, Fig. 1b shows XRD pattern of Cr_2O_3 thin film. The diffraction peaks at 2θ of 33.50°, 41.38°, 43.66° are assigned to (104), (113), (202) planes of the Cr_2O_3 crystal lattice respectively, which reveals the formation of rhombohedral crystal symmetry [JCPDS card no. 81-0314]. The peaks originated due to SS substrate are indicated by (SS). Figure 1c show XRD spectra of layered PPy/Cr_2O_3 layered structure thin film. The XRD spectrum shows all the peaks corresponding to Cr_2O_3 thin film only and no peak corresponding to any impurity phase was seen in the XRD spectrum.

3.2 Fourier transform infrared (FTIR) spectroscopy

Figure 2 shows the FTIR spectrum of layered PPy/Cr_2O_3 thin film deposited on stainless steel substrate. The powder collected from the deposited films was characterized by FTIR spectroscopy in the range of 500–4000 cm^{-1}. The peak observed at 3440 cm^{-1} corresponds to –OH vibration band corresponding to water. The characteristic peaks observed at 2933 and 2855 cm^{-1} correspond to N–H bond present in aromatic amines [32]. The peak observed at 1628 cm^{-1} belongs to C–C backbone stretching [33]. The peak 1177 cm^{-1} correspond the C–N stretching vibrations [34]. These characteristic peaks confirmed the formation of polypyrrole in PPy/Cr_2O_3 thin films.

3.3 Surface morphological studies

Figure 3a–c shows the SEM images of PPy, Cr_2O_3 and PPy/Cr_2O_3 thin films respectively. Figure 3a shows SEM images of PPy thin film. The microstructure of PPy thin film shows cauliflower like structure [35]. Figure 3b shows the SEM images of Cr_2O_3 thin film, it can be seen that the Cr_2O_3 thin films exhibits compact, smooth, sponge like morphology [36]. Figure 3c shows the SEM images of Cr_2O_3 particles deposited on PPy thin film. The microstructure of PPy/Cr_2O_3 thin film shows the Cr_2O_3 particles are diffuse inside the microstructure of PPy thin films. The films are uniformly deposited. Thus, the layered PPy/Cr_2O_3 thin film gives combined features of PPy and Cr_2O_3 thin films which are feasible for supercapacitor study. The layered compositions consist of PPy and Cr_2O_3, which are stacked to form unit arrangement, which offer a different microstructure to improve strength of active sites for promoting electrolyte/electrode reactions. Improved microstructure is a potential candidate for supercapacitor application, will provides rigidity; it possesses loosely connected PPy/Cr_2O_3 layered structure along with advantageous for the electrolyte ions to access the active materials. Hence, results in Faradaic reaction, which may improve the stability in capacitive performance [37].

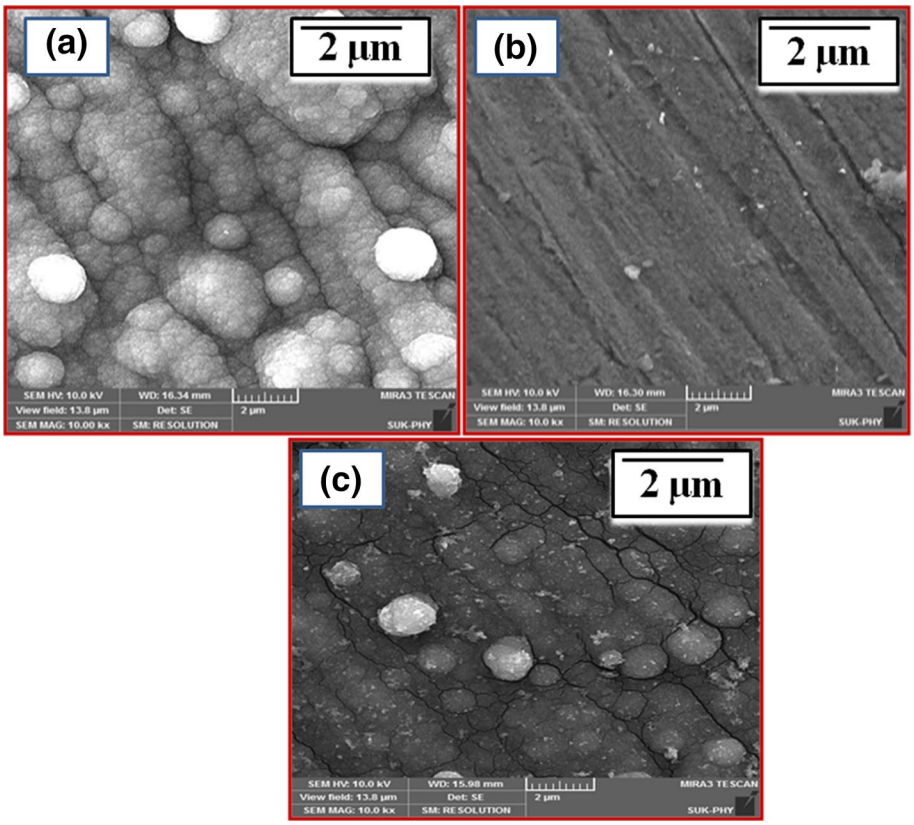

Fig. 3 Scanning electron microscope images of **a** PPy thin film, **b** Cr_2O_3 thin film and **c** PPy/Cr_2O_3 thin film

3.4 Cyclic voltammetry studies

Cyclic voltammetry is a fascinating tool to analyze the capacitive performance of prepared electrodes. Large amount of current, symmetric in anodic and cathodic path and rectangular types of waveforms remarks ideal supercapacitive behaviour of materials. Figure 4A (a–c) shows typical cyclic voltammetry curves of PPy, Cr_2O_3 and PPy/Cr_2O_3 electrodes within the potential window of −1.0 to +1.0 V versus SCE at scan rate of 5 mV s^{-1} in aqueous

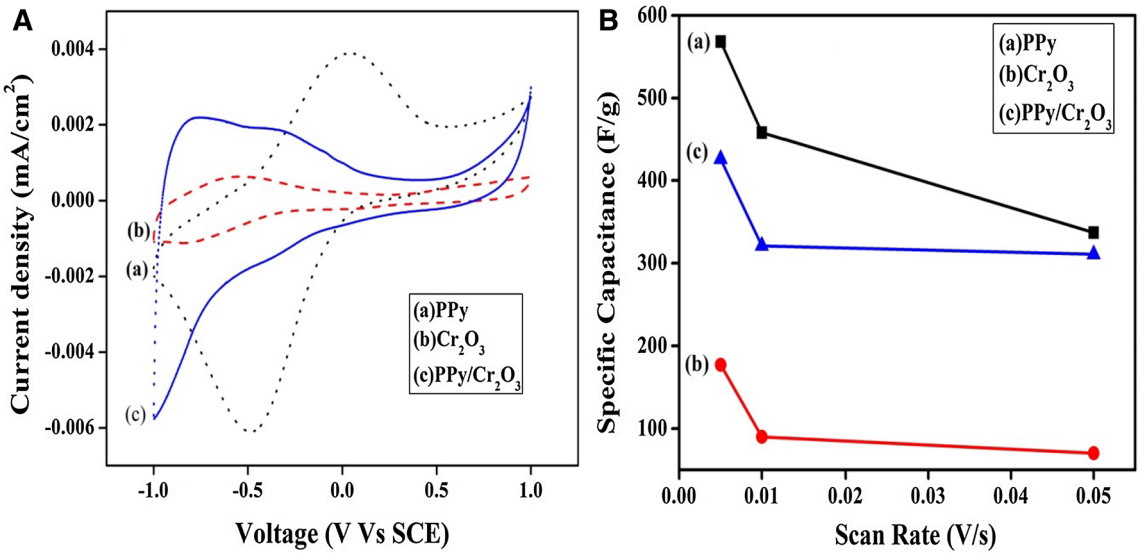

Fig. 4 **A** Cyclic voltammetry of (*a*) PPy thin film (*b*) Cr_2O_3 thin film and (*c*) PPy/Cr_2O_3 thin film at 5 mV s^{-1} scan rate. **B** Specific capacitance versus scan rates of PPy, Cr_2O_3 and PPy/Cr_2O_3 thin films

0.5 M Na_2SO_4 electrolyte. The Cr_2O_3 electrode shows very low current density as shown in Fig. 4A (b) due to its non-electroactive nature and low area under curve as compared to PPy electrode. It is seen that current density of layered PPy/Cr_2O_3 thin films are rising. This is may be due to reduction of internal resistance between less conducting Cr_2O_3 adhered on conducting PPy chains. Hence specific capacitance of layered PPy/Cr_2O_3 thin films is improved as compared to Cr_2O_3 thin film. The Cr_2O_3 electrode shows oxidation peaks at −0.39 and +0.7 V versus SCE. In this potential window Cr(III) oxidises to Cr(VI) via no. of oxidation states. Also it reduces from Cr(VI) to Cr(III) via no. of reduction states such as Cr(VI) to Cr(V) and Cr(V) to Cr(III). The reduction of Cr(V) to Cr(III) is fast and stable state. The CV shows the reduction peaks at +0.21 and −0.42 V versus SCE which corresponds to oxidised Cr(VI) reduces from Cr(VI) to Cr(III) [38–40].

Figure 4A (a) shows a pair of redox peaks of polypyrrole thin film electrode within the potential range −1.0 to +1.0 V versus SCE with scan rate 5 mV s^{-1}. The CV shows the oxidation peak at +0.04 V versus SCE, which corresponds to over oxidised polypyrrole back bone. In the reverse scan the reduction peak is observed at −0.49 V versus SCE, which corresponds to reduction of polypyrrole backbone. Also, during reduction process of polypyrrole there may be insertion of SO_4^{-2} ions into polymer chain and hence current density increases in the reverse scan. Figure 4A (c) shows CV of PPy/Cr_2O_3 layered structure. The layered structure strongly differentiates the CV's obtained from parent electrodes. There is shifting in the oxidation and reduction potentials of the species in the layered structure. The oxidation peak at −0.74 V versus SCE corresponds to oxidation of Cr(III) species. Also, the oxidation peak at −0.28 V versus SCE corresponds to oxidation of PPy chain. In the reverse scan the reduction peak is observed at +0.63 V versus SCE corresponds to reduction of Cr species and the peak at −0.36 V versus SCE is due to the reduction of PPy chain. Specific capacitance values are to be determined by using the formula reported in earlier reference [29]. The PPy, Cr_2O_3 and layered PPy/Cr_2O_3 thin films shows maximum specific capacitance of 565, 177 and 426 F g^{-1} respectively at the scan rate of 5 mV s^{-1} versus SCE.

Figure 4B (a–c) shows dependence of specific capacitance vs scan rates of PPy, Cr_2O_3 and layered PPy/Cr_2O_3 thin films in aqueous 0.5 M Na_2SO_4 electrolyte at scan rate of 5, 10, 50 mV s^{-1}. From the Fig. 4B (a–c), it can be seen that as scan rate increases specific capacitance decreases. The decrease in specific capacitance proposes that; at higher scan rates, the presence of inner active sites that can incomplete the redox transitions. These imperfect redox transitions may be because of the diffusion effect of ions within the electrode. Hence, the specific capacitance obtained at the low scan rate is indication to be close to that for full utilization of the electrode material [41].

3.5 Electrochemical stability studies

The electrochemical cycling stability of the PPy, Cr_2O_3 and layered PPy/Cr_2O_3 thin film electrodes were calculated by repeating the CV test for 1000 cycles at 100 mV s^{-1} scan rate in aqueous 0.5 M Na_2SO_4 electrolyte solution. The variation of specific capacitance with cycle number for the electrodes is shown in Fig. 5a–c, which shows that specific capacitance decreases with increasing the cycle number. The capacitance retained ratios after 1000 cycles (capacitance at the 1000th cycle/capacitance at the 1st cycle) of the PPy, Cr_2O_3 and PPy/Cr_2O_3 electrodes were 78, 81 and 89%, respectively. This implies that stability of PPy thin film is improved with layered structure of Cr_2O_3 thin film. The layered structure PPy/Cr_2O_3 can provide better electronic conducting channel, due to excellent conductivity of PPy. Also, PPy efficiently provide electron transfer to improve electrochemical performance of layered structure PPy/Cr_2O_3. This indicates that PPy/Cr_2O_3 layered composite thin film possesses excellent long-term recycling capability.

3.6 Galvanostatic charging–discharging (GCD) studies

To analyse the specific power and specific energy of prepared PPy, Cr_2O_3 and the layered PPy/Cr_2O_3 electrodes, a galvanostatic charge–discharge (GCD) study was carried out in aqueous 0.5 M Na_2SO_4 electrolyte solution at a current density of 0.5 mA cm^{-2} over the potential window of −1.0 to +1.0 V as shown in Fig. 6a–c. The values of specific capacitance (SC), specific energy (SE) and specific power (SP) at current density 0.5 mA g^{-1} were calculated from following formulae (1, 2, 3) respectively.

$$SC = \frac{I_d \times T_d}{\Delta V \times W} \tag{1}$$

$$SE = \frac{SC \times \Delta V^2}{2} \tag{2}$$

and

$$SP = \frac{SE^2}{T_d} \tag{3}$$

where I_d—discharge current, T_d—discharge time, V—potential window and W—mass of active material.

Table 1 shows the variation of columbic efficiency, specific capacitance, specific power and specific energy. From Table 1, it could be seen that the performance of Cr_2O_3 thin film is improved and enhance with the PPy thin film. The specific capacitance of PPy, Cr_2O_3 and PPy/Cr_2O_3 thin

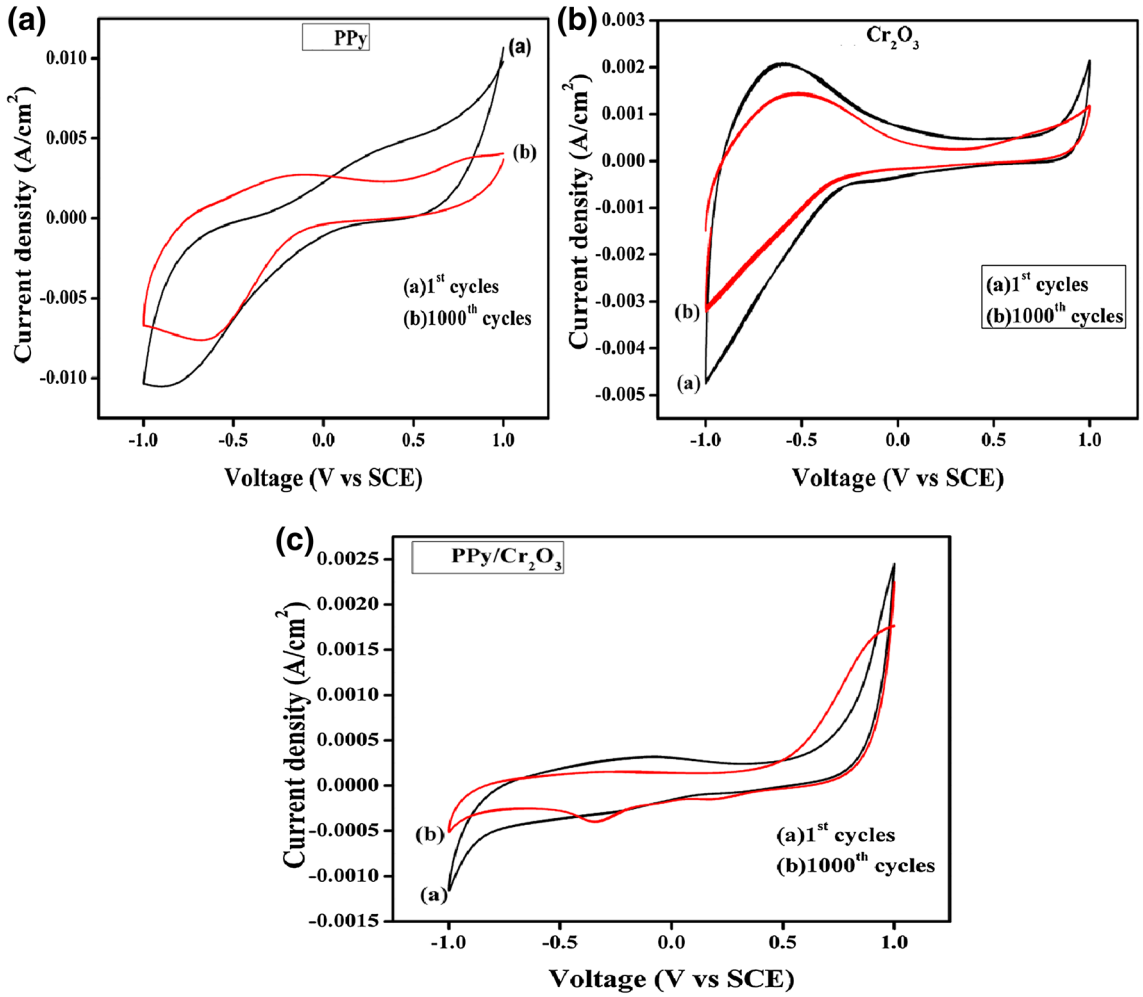

Fig. 5 Electrochemical stability of **a** PPy thin film, **b** Cr_2O_3 thin film and **c** PPy/Cr_2O_3 thin film

films are 466, 118.36 and 392 F g^{-1} respectively. The specific capacitance obtained from CV and GCD techniques are comparable. The coulombic efficiency and specific power of PPy/Cr_2O_3 thin film is greater than that of Cr_2O_3 and PPy thin film. By creating nanosized porosity between Cr_2O_3 and PPy, open transport paths and a more fast access of the electrolyte to the active surface of Cr_2O_3 are provided, which consequently result in a low ion transport resistance in PPy/Cr_2O_3. In addition, the layered structure helps to reduce the resistance of effective electrochemical penetration of ions through the PPy and to easily access the internal surface of PPy. Similar results have been reported for polymer–metal oxide composites [42].

Further, specific capacitance and specific energy of PPy/Cr_2O_3 is greater as compared to Cr_2O_3. Therefore, PPy/Cr_2O_3 bilayer thin film shows improved performance than PPy and Cr_2O_3 thin films.

3.7 Electrochemical impedance spectroscopy (EIS) studies

Electrochemical Impedance Spectroscopy (EIS) measurements of the PPy, Cr_2O_3 and the layered PPy/Cr_2O_3 electrodes were performed within the frequency range 10^2–10^5 Hz. Figure 7a–c shows the Nyquist plot for the PPy, Cr_2O_3 and PPy/Cr_2O_3 thin film in the in aqueous 0.5 M Na_2SO_4 solution as electrolyte. The Nyquist plots of PPy and PPy/Cr_2O_3 thin film shows semi-circle nature at high frequency region and straight line in the low frequency region indicating capacitive behaviour of the prepared electrodes, while the Nyquist plot chromium oxide film electrode shows double semi-circle which indicates poor performance of charge storage. The value of charge transfer resistance (R_{ct}) for PPy, Cr_2O_3 and layered PPy/

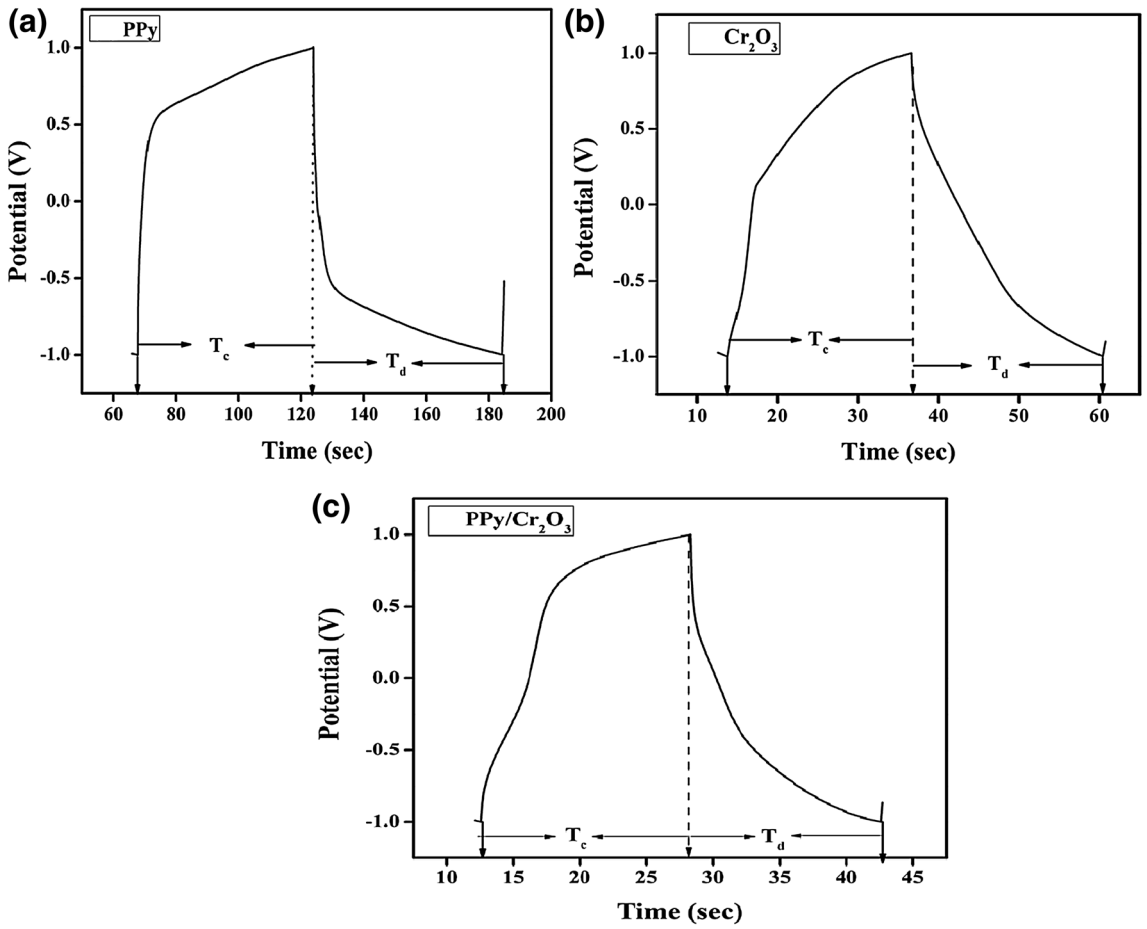

Fig. 6 Charging–discharging curves of **a** PPy thin film, **b** Cr_2O_3 thin film and **c** PPy/Cr_2O_3 thin film

Table 1 Columbic efficiency, specific capacitance, specific energy and specific power for PPy, Cr_2O_3 and PPy/Cr_2O_3 at constant current density of 0.5 mA cm^{-2}

Electrodes	Coulombic efficiency in (%)	Specific capacitance in (F g^{-1})	Specific energy in (Wh kg^{-1})	Specific power in (kW kg^{-1})
PPy	86.63	466	48.68	14.54
Cr_2O_3	95.41	118.36	13.1	20
PPy/Cr_2O_3	97	392	49.57	49.75

Cr_2O_3 electrodes were 4.76, 3.16 and 2.98 Ω respectively. From the Fig. 7b–c; it is clear that the second semicircle in the low frequency region for chromium oxide changes to straight line for layered PPy/Cr_2O_3 structure. This indicates that the layered structure has improved charge storage ability. The R_{ct} of the layered PPy/Cr_2O_3 electrode is smaller than that of the PPy and Cr_2O_3 electrodes. The low value R_{ct} of the layered PPy/Cr_2O_3 electrode is due to inclusion of Cr_2O_3 on PPy chain which facilitate a more rapidly cation insertion/extraction process into/from the PPy chain, which leads to better electrochemical performance.

4 Conclusions

In summary, three different electrode materials such as PPy, Cr_2O_3 and layered PPy/Cr_2O_3 were successfully prepared by galvanostatic electrodeposition method. SEM micrographs of the thin film show porous nature of the electrode materials which are feasible for easy access of protons during

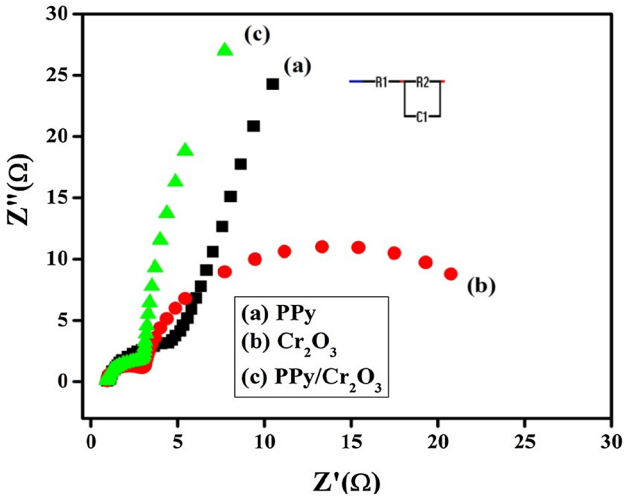

Fig. 7 Electrochemical impedance spectroscopy (Nyquist plot) of (*a*) PPy thin film, (*b*) Cr_2O_3 thin film and (*c*) PPy/Cr_2O_3 thin film

intercalation and de-intercalation. It is observed that PPy/Cr_2O_3 layered thin film give higher value of specific capacitance, specific power, specific energy and coulombic efficiency than individual PPy and Cr_2O_3 thin film. Also the cycling stability of PPy/Cr_2O_3 layered thin film electrode is better than PPy and Cr_2O_3 thin films. The EIS study remarks that PPy/Cr_2O_3 layered thin film electrode provides very low impedance which can be easily access charge carriers from intercalation and de-intercalation. The synergistic effect of layered PPy/Cr_2O_3 composite contributes to enhancing the supercapacitive properties of electrode material in terms of high specific capacitance, cycle stability and coulombic efficiency. Thus, amongst all the electrodes, galvanostatically deposited PPy/Cr_2O_3 layered thin film is one of the superior candidate for supercapacitor application.

Acknowledgements Authors S.L. Kadam and S.B. Kulkarni are thankful to Department of Atomic Energy-Board of Research in Nuclear Sciences (DAE-BRNS) for financial support through Grant No. 2013/34/BRNS/2691.

References

1. S. Kandalkar, D. Dhawale, C. Kim, C. Lokhande, Chemical synthesis of cobalt oxide thin film electrode for supercapacitor application. Synth. Met. **160**, 1299–1302 (2010)
2. C. Heymans, S. Walker, S. Young, M. Fowler, Economic analysis of second use electric vehicle batteries for residential energy storage and load-leveling. Energy Policy **71**, 22–30 (2014)
3. R.B. Rakhi, H.N. Alshareef, Enhancement of the energy storage properties of supercapacitors using graphene nanosheets dispersed with metal oxide-loaded carbon nanotubes. J. Power Sources **196**, 8858–8865 (2011)
4. B.E. Conway, *Electrochemical Supercapacitors, Scientific Fundamentals and Technological Applications*. (Kluwer Academic/Plenum Press, New York, 1999)
5. J.S. Shaikh, R.C. Pawar, R.S. Devan, Y.R. Ma, P.P. Salvi, S.S. Kolekar, P.S. Patil, Synthesis and characterization of Ru doped CuO thin films for supercapacitor based on Bronsted acidic ionic liquid. Electroch. Act. **56**, 2127–2134 (2011)
6. M. Kalaji, P.J. Murphy, G.O. Williams, The study of conducting polymers for use as redox supercapacitors. Synth. Met. **102**, 1360–1361 (1999)
7. K.R. Prasad, K. Koga, N. Miura, Electrochemical deposition of nanostructured indium oxide: high-performance electrode material for redox supercapacitors. Chem. Mater. **16**, 1845–1947 (2004)
8. L. Fan, J. Maier, High performance polypyrrole electrode materials for redox supercapacitors. Electrochem. Commun. **8**, 937–940 (2006)
9. J.K. Lee, H.M. Pathan, K.D. Jung, Electrochemical capacitance of nanocomposite films formed by loading carbon nanotubes with ruthenium oxide. J. Power. Sources **159**, 1527–1531 (2006)
10. Z. Yu, B. Duong, D. Abbott, J. Thomas, Highly ordered MnO_2 nanopillars for enhanced supercapacitor performance. Adv. Mater. **25**, 3302 (2013)
11. A.D. Jagadale, V.S. Kumbhar, C.D. Lokhande, Supercapacitive activities of potentiodynamically deposited nanoflakes of cobalt oxide (Co_3O_4) thin film electrode. J. Colloid Interf. Sci. **406**, 225–230 (2013)
12. L. Gu, Y. Wang, R. Lu, L. Guan, X. Peng, J. Sha, Anodic electrodeposition of a porous nickel oxide-hydroxide film on passivated nickel foam for supercapacitors. J. Mater. Chem. A **2**, 7161 (2014)
13. X. Xu, J. Wu, N. Yang, H. Na, L. Li, Cr_2O_3: novel supercapacitor electrode material with high capacitive performance. J. Gao Mater. Lett. **142**, 172–175 (2015)
14. Y.F. Zhang, Z.S. Lou, Q.W. Chen, Chin. J. Inorg. Chem. **1–4**, 2097 (2004)
15. T.V.M. Rao, Y. Yang, A. Sayari, Ethane dehydrogenation over pore-expanded mesoporous silica supported chromium oxide: 1. Catalysts preparation and characterization. J. Mol. Catal. A **301**, 152–158 (2009)
16. T.V.M. Rao, E. Zahidi, A. Sayari', Ethane dehydrogenation over pore-expanded mesoporous silica supported chromium oxide: 2.Catalytic properties and nature of active sites. J. Mol. Catal. A **301**, 159–165 (2009)
17. G. Wang, L. Zhang, J. Deng, H. Dai, H. He, C. Tong, Preparation, characterization and catalytic activity of chromia supported on SBA-15 for the oxidative dehydrogenation of isobutene. Appl. Catal. A **355**, 192–201 (2009)
18. U. Balachandran, R.W. Siegel, Y.X. Liao, T.R. Askew, Synthesis, sintering, and magnetic properties of nanophase Cr_2O_3. Nanostruct. Mater. **550**, 5–12 (1995)
19. C.J. Cantalini, Cr_2O_3, WO_3 single and Cr/W binary oxide prepared by physical methods for gas sensing applications. J. Eur. Ceram. Soc. **24**, 1421–1424 (2004)
20. P. Li, H.B. Xu, Y. Zhang, Z.H. Li, S.L. Zheng, Y.L. Bai, The effects of Al and Ba on the colour performance of chromic oxide green pigment. Dyes Pigm. **80**, 287–291 (2009)
21. X. Pang, K. Gao, F. Luo, Y. Emirov, A.A. Levin, A.A. Volinsky, Investigation of micro structure and mechanical properties of multi-layer Cr/Cr_2O_3 coatings. Thin Solid Films **517**, 1922–1927 (2009)
22. X. Hou, K.L. Choy, Synthesis of Cr_2O_3-based nanocomposite coatings within corporation of inorganic fullerene-like nanoparticles. Thin Solid Films **516**, 8620–8624 (2008)
23. D.W. Kim, S.I. Shin, J.D. Lee, S.G. Oh, Preparation of chromia nanoparticle by precipitation-gelation reaction. Mater. Lett. **58**, 1894–1898 (2004)

24. V. Teixeira, E. Sousa, M.F. Costa, C. Nunes, L. Rosa, M.J. Carvalho, M. Collares-Pereira, E. Roman, J. Gago, Spectrally selective composite coatings of Cr-Cr_2O_3 and Mo-Al_2O for solar energy application. Thin Solid Films **392**, 320–326 (2001)
25. L. Yuan, C. Wan, L. Zhao, Facial in-situ synthesis of MnO_2/PPy composite for supercapacitor. Int. J. Electrochem. Sci. **10**, 9456–9465 (2015)
26. X. Yan, K. Xu, R. Zou, J. Hu, A hybrid electrode of Co_3O_4@PPy core/shell nanosheet arrays for high-performance supercapacitors. Nano-Micro Lett. **8**(2), 143–150 (2016)
27. Z.L. Wang, R. Guo, L.X. Ding, Y.X. Tong, G.R. Li, Controllable template assisted electrodeposition of single- and multi-walled nanotube arrays for electrochemical energy storage. Sci. Rep. **3** (2013). doi:10.1038/srep01204
28. M.S. Kim, J.H. Park, Polypyrrole/titanium oxide nanotube arrays composites as an active material for supercapacitors. J. Nanosci. Nanotechnol. **11**, 4522–4526 (2011)
29. P.M. Kharade, S.M. Mane, S.B. Kulkarni, P.B. Joshi, D.J. Salunkhe, Ground nut seed like hydrophilic polypyrrole based thin film as a supercapacitor electrode. J. Mater. Sci. **27**, 3499–3505 (2016)
30. D.P. Dubal, S.V. Patil, W.B. Kim, C.D. Lokhande, Supercapacitors based on electrochemically deposited polypyrrole nanobricks. Mater. Lett. **65**, 2628–2631 (2011)
31. S.P. Palaniappan, P. Manisankar, Rapid synthesis of polypyrrole nanospheres by greener mechanochemical route. Mater. Chem. Phys. **122**, 15–17 (2010)
32. C. Yang, T. Wang, P. Liu, H. Shi, D. Xue, Preparation of well-defined blackberry-like polypyrrole/fly ash composite microspheres and their electrical conductivity and magnetic properties. Solid State Mater. Sci. **13**, 112 (2009)
33. S. Bose, N.H. Kim, T. Kuila, K. Lau, J.H. Lee, Electrochemical performance of a graphene–polypyrrole nanocomposite as a supercapacitor electrode. Nano-technology **22**, 295202 (2011)
34. X. Yang, L. Li, Polypyrrole nanofibers synthesized via reactive template approach and their NH_3 gas sensitivity. Synth. Met. **160**, 1365 (2010)
35. J.V. Thombare, M.C. Rath, S.H. Han, V.J. Fulari, The influence of monomer concentration on the optical properties of electrochemically synthesized polypyrrole thin films. J. Semicond. **34**, 103002–103006 (2013)
36. S. Eugénio, C.M. Rangel, R. Vilar, S. Quaresma, Electrochemical aspects of black chromium electrodeposition from 1-butyl-3-methylimidazoliumtetrafluoroborate ionic liquid. Electrochim. Acta **56**, 10347–10352 (2011)
37. S.B. Kulkarni, A.D. Jagadale, V.S. Kumbhar, R.N. Bulakhe, S.S. Joshi, C.D. Lokhande, Potentiodynamic deposition of composition influenced $Co_{1-x}Ni_x$ LDHs thin film electrode for redox supercapacitors. Int. J. Hydrog. Energy **38**, 4046–4053 (2013)
38. C.M. Welch, O. Nekrassova, R.G. Compton, Reduction of hexavalent chromium at solid electrodes in acidic media: reaction mechanism and analytical applications. Talanta **65**, 74–80 (2005)
39. P. Skołuda, The oxidation of trivalent chromium at Au (111) electrode. Electrochem. Commun. **9**, 405–408 (2007)
40. C.M. Welch, M.E. Hyde, O. Nekrassova, R.G. Compton, The oxidation of trivalent chromium at polycrystalline gold electrodes. Phys. Chem. Chem. Phys. **6**, 153–3159 (2004)
41. D.P. Dubal, D.S. Dhawale, R.R. Salunkhe, S.M. Pawar, C.D. Lokhande, A novel chemical synthesis and characterization of Mn_3O_4 thin films for supercapacitor application. Appl. Surf. Sci. **256**, 4411–4416 (2010)
42. L. Chen, Z. Song, G. Liu, J. Qiu, C. Yu, J. Qin, L. Ma, F. Tian, W. Liu, Synthesis and electrochemical performance of polyaniline-MnO_2 nanowire composites for supercapacitors. J. Phys. Chem. Solid **74**, 360–365 (2013)

Terms and Conditions

Springer Nature journal content, brought to you courtesy of Springer Nature Customer Service Center GmbH (“Springer Nature”).
Springer Nature supports a reasonable amount of sharing of research papers by authors, subscribers and authorised users (“Users”), for small-scale personal, non-commercial use provided that all copyright, trade and service marks and other proprietary notices are maintained. By accessing, sharing, receiving or otherwise using the Springer Nature journal content you agree to these terms of use (“Terms”). For these purposes, Springer Nature considers academic use (by researchers and students) to be non-commercial.
These Terms are supplementary and will apply in addition to any applicable website terms and conditions, a relevant site licence or a personal subscription. These Terms will prevail over any conflict or ambiguity with regards to the relevant terms, a site licence or a personal subscription (to the extent of the conflict or ambiguity only). For Creative Commons-licensed articles, the terms of the Creative Commons license used will apply.
We collect and use personal data to provide access to the Springer Nature journal content. We may also use these personal data internally within ResearchGate and Springer Nature and as agreed share it, in an anonymised way, for purposes of tracking, analysis and reporting. We will not otherwise disclose your personal data outside the ResearchGate or the Springer Nature group of companies unless we have your permission as detailed in the Privacy Policy.
While Users may use the Springer Nature journal content for small scale, personal non-commercial use, it is important to note that Users may not:

1. use such content for the purpose of providing other users with access on a regular or large scale basis or as a means to circumvent access control;
2. use such content where to do so would be considered a criminal or statutory offence in any jurisdiction, or gives rise to civil liability, or is otherwise unlawful;
3. falsely or misleadingly imply or suggest endorsement, approval , sponsorship, or association unless explicitly agreed to by Springer Nature in writing;
4. use bots or other automated methods to access the content or redirect messages
5. override any security feature or exclusionary protocol; or
6. share the content in order to create substitute for Springer Nature products or services or a systematic database of Springer Nature journal content.

In line with the restriction against commercial use, Springer Nature does not permit the creation of a product or service that creates revenue, royalties, rent or income from our content or its inclusion as part of a paid for service or for other commercial gain. Springer Nature journal content cannot be used for inter-library loans and librarians may not upload Springer Nature journal content on a large scale into their, or any other, institutional repository.
These terms of use are reviewed regularly and may be amended at any time. Springer Nature is not obligated to publish any information or content on this website and may remove it or features or functionality at our sole discretion, at any time with or without notice. Springer Nature may revoke this licence to you at any time and remove access to any copies of the Springer Nature journal content which have been saved.
To the fullest extent permitted by law, Springer Nature makes no warranties, representations or guarantees to Users, either express or implied with respect to the Springer nature journal content and all parties disclaim and waive any implied warranties or warranties imposed by law, including merchantability or fitness for any particular purpose.
Please note that these rights do not automatically extend to content, data or other material published by Springer Nature that may be licensed from third parties.
If you would like to use or distribute our Springer Nature journal content to a wider audience or on a regular basis or in any other manner not expressly permitted by these Terms, please contact Springer Nature at

onlineservice@springernature.com